

Cadmium Resistance, Microbial Biosorptive Performance and Mechanisms of a Novel Biocontrol Bacterium *Paenibacillus* sp. LYX-1

Yixin Luo

Zhejiang University

Min Liao (✉ liaomin@zju.edu.cn)

Zhejiang University <https://orcid.org/0000-0001-9078-204X>

Yuhao Zhang

Zhejiang University

Na Xu

Zhejiang University

Xiaomei Xie

Zhejiang University

Qiyang Fan

Zhejiang University

Research Article

Keywords: *Paenibacillus* sp., Cd resistance, Biosorption, Mechanism

Posted Date: November 16th, 2021

DOI: <https://doi.org/10.21203/rs.3.rs-1003036/v1>

License: © ⓘ This work is licensed under a Creative Commons Attribution 4.0 International License.

[Read Full License](#)

1 **Title Page**

2

3 **The Full Title:** Cadmium resistance, microbial biosorptive performance and
4 mechanisms of a novel biocontrol bacterium *Paenibacillus* sp. LYX-1

5 **Name of authors :** YiXin Luo ^{a,b}, Min Liao ^{a,b*}, Yuhao Zhang ^{a,b}, Na Xu ^{a,b}, Xiaomei
6 Xie ^{a,c*}, Qiyang Fan ^{a,c}

7 a. College of Environmental and Resource Science, Zhejiang University, Yuhangtang
8 Road No.866, Hangzhou 310058 China

9 b. Zhejiang Provincial Key Laboratory of Agricultural Resources and Environment,
10 Yuhangtang Road No.866, Hangzhou 310058, China

11 c. National Demonstration Center for Experimental Environmental and Resources
12 Education (Zhejiang University), Yuhangtang Road No.866, Hangzhou 310058, China

13 **First author:** YiXin Luo.

14 ***Corresponding author:** Min Liao; Xiaomei Xie

15 **E-mail:** liaomin@zju.edu.cn; xiexiaomei@zju.edu.cn

16 **Telephone:** +86-15372058710

17 **Fax:** +86-571-8892719

18

19 **Financial support:** This work was supported by the National Key Research and
20 Development Project of China (2018YFC1800403) and the National Natural Science
21 Fund of China (41571226)

22

23 **Cadmium resistance, microbial biosorptive performance**
24 **and mechanisms of a novel biocontrol bacterium**

25 ***Paenibacillus* sp. LYX-1**

26 Yixin Luo ^{a,b}, Min Liao ^{a,b*}, Yuhao Zhang ^{a,b}, Na Xu ^{a,b}, Xiaomei Xie ^{a,c*}, Qiyan Fan ^{a,c}

27 a. *College of Environmental and Resource Science, Zhejiang University, Yuhangtang Road No.866,*

28 *Hangzhou 310058 China*

29 b. *Zhejiang Provincial Key Laboratory of Agricultural Resources and Environment, Yuhangtang*

30 *Road No.866, Hangzhou 310058, China*

31 c. *National Demonstration Center for Experimental Environmental and Resources Education*

32 *(Zhejiang University), Yuhangtang Road No.866, Hangzhou 310058, China*

33 ** Corresponding author, E-mail: liaomin@zju.edu.cn; xiexiaomei@zju.edu.cn*

34 **Abstract:** In order to explore whether the newly discovered biocontrol strain *Paenibacillus* sp.,
35 LYX-1 having antagonistic effect on peach brown rot was resistant to Cd²⁺, a series of growth of
36 strain LYX-1 under different Cd concentration and biosorption experiments were conducted to
37 living and dead strain LYX-1. Meanwhile, the Cd²⁺ resistance and biosorption mechanisms were
38 further identified by Cd-resistant genes, TEM, SEM-EDS, FTIR and XPS analysis. The results
39 showed that strain LYX-1 could resist 50 mg/L Cd²⁺ and the adsorption process of both living and
40 dead strain LYX-1 all satisfied the pseudo-second kinetic equation. Under pH 8.0 and at a dose of
41 1.0 g/L strain, the removal capacities of living and dead cells were as high as 90.39% and 75.67%
42 at 20 mg/L Cd²⁺, respectively. For the adsorption isotherm test, results revealed that both Langmuir
43 (R²=0.9704) and Freundlich (R²=0.9915) model could describe the Cd²⁺ biosorption well for living
44 strain LYX-1. The maximum equilibrium biosorption capacities of living and dead biomass were
45 30.6790 and 24.3752 mg/g, respectively. The adsorption mechanism was controlled by
46 chemisorption with -OH, -NH, -C=O, O=C-O, C-N, S²⁻ and phosphate functional groups on the cell
47 surface of strain LYX-1, which were further identified by XPS. The insignificant biosorption
48 difference of living and dead biomass was caused by CzcD gene in strain LYX-1 detoxifying

49 cadmium through the heavy metal efflux system. The above results indicated that strain LYX-1 had
50 higher tolerance and fixed capacity to Cd²⁺.

51 **Keywords:** *Paenibacillus* sp.; Cd resistance; Biosorption; Mechanism

52 **1. Introduction**

53 Heavy metals (HMs) are the main pollutants in the development of mineral
54 resources, textile, fertilizer manufacturing, metal smelting and processing(Jin et al.
55 2019). Cadmium (Cd) designated as one of the priority pollutants controlled by many
56 countries can participate in food chain cycle, accumulate in the organism and eventually
57 cause irreversible tubular damage in kidney after it enters the environment(Jin et al.
58 2020). Therefore, effective treatment of heavy metal Cd pollution in soil and water has
59 become an important issue that needs to be solved urgently in the field of environmental
60 protection today.

61 Compared with conventional chemical precipitation, electrolysis, reverse osmosis,
62 ion exchange, etc., microbial adsorption had significant advantages, mainly including
63 high efficiency, abundant raw materials, coupled with high chemical activity(Li et al.
64 2018, Shi et al. 2021, Sun et al. 2020). Additionally, in domestic and international
65 literatures, more and more strains employed as environmentally friendly biomasses
66 have been applied in the removal of metal ions, such as *Comamonas* sp. XL8(Shi et al.
67 2021), *Enterbacter* sp. DNB-S2(Sun et al. 2020), *Serratia liquefaciens* CL-1 and
68 *Bacillus thuringiensis* X3(Han et al. 2018). Besides, numerous evidences have proved
69 that biological cell components (e.g., cell wall polysaccharides, proteins, carboxyl in
70 lipid molecules, hydroxyl, carbonyl, phosphoryl, sulfhydryl) realized the accumulation
71 and purification of heavy metals through chelation, ion exchange, biosorption,
72 inorganic micro-precipitation, redox and diffusion(Huang et al. 2014, Özdemir et al.
73 2009, Tan et al. 2020, Zhou et al. 2018).

74 At present, the environment polluted by HMs is widespread, and there are few
75 reports on the adaptability of the currently used biocontrol bacterium as microbial
76 materials for heavy metal pollution control under the stress of HMs. The search and
77 discovery of biocontrol bacterium that have high tolerance and immobilization to HMs

78 is great significance to the restoration and utilization of heavy metal contaminated soils.

79 *Paenibacillus* sp. is a kind of significant disease biological control microorganism,
80 which due to their ability to produce-variety of enzymes of degrading the cell wall, e.g.
81 chitinases, cellulases, proteases and β -1,3-glucanases(Hao et al. 2017). In the previous
82 study, *Paenibacillus* sp. showed diverse antagonistic activities against five
83 phytopathogenic fungi (*Fusarium graminearum*, *Magnaporthe oryzae*, *Rhizoctonia*
84 *solani*, *Sclerotinia sclerotiorum*, and *Botrytis cinerea*)(Ali et al. 2020). Researches over
85 the past decades showed that *Paenibacillus* sp. could produce a variety of antibiotics,
86 polymyxin, hydrolases and other antagonistic substances(Ali et al. 2020, Araujo et al.
87 2020), which was one of the important mechanisms for the biocontrol of *Paenibacillus*
88 sp.(Hao et al. 2017). *Paenibacillus* sp. can not only offer protection against bacteria,
89 fungi, nematodes and viruses, but also has advantages of non-pathogenicity, non-
90 toxicity, good environmental compatibility, less residue, safety for humans and animals.
91 Nevertheless, the survival of biocontrol bacterium employed for prevention and control
92 of plant diseases are prone to be threatened by toxic Cd, pests and diseases in composite
93 pollutant sites(Olaniran et al. 2013). Therefore, finding a *Paenibacillus* sp. with high
94 tolerance and fixation capacity for Cd is of great significance for the simultaneous
95 control of soil Cd pollution and plant rhizosphere disease. However, relevant studies
96 are rarely reported.

97 In present work, a novel biocontrol strain *Paenibacillus* sp. LYX-1 having
98 antagonistic to peach brown rot and higher Cd resistance was isolated from soil in
99 peach orchard. The Cd resistance, microbial biosorptive performance and mechanisms
100 of *Paenibacillus* sp. LYX-1 were studied, including (1) investigate the Cd resistance
101 of biocontrol *Paenibacillus* sp. LYX-1, (2) compare the biosorption process of living
102 and dead biosorbents, closer to the real-world scenarios where nutrients are deficient,
103 (3) describe the biosorption performance of living and dead cells via kinetic and
104 isotherm models and (4) explore the Cd²⁺ resistance and removal mechanisms through
105 HMs gene coding, TEM, SEM-EDS, FTIR and XPS analysis. The objective of such
106 work is to provide a theoretical basis focusing a *Paenibacillus* sp. LYX-1 with higher
107 Cd resistance to realize the simultaneous control of soil Cd pollution and plant

108 rhizosphere disease in Cd stress soil in future.

109 **2. Materials and methods**

110 ***2.1 Isolation and identification of biocontrol strain***

111 Biocontrol strain was isolated as following steps. Ten g of rhizosphere soil in peach
112 orchard in Fenghua city, Zhejiang province, China was initially suspended in 90 mL of
113 sterile water and incubated at 180rpm, 30°C for 1h. The gradient dilution method was
114 used to dilute the soil into soil suspensions with sterile water. 0.1mL 10⁻⁴, 10⁻⁵ and 10⁻⁶
115 gradient dilutions were applied to Luria-Bertani's (LB) agar plate consisted of 10 g/L
116 tryptone, 5.0 g/L yeast extract, 10.0 g/L NaCl and 20.0 g/L agar. There replicates for
117 each gradient were incubated at 30°C. (1) Primer screening: 6mm diameter peach brown
118 rot fungus taken by a hole puncher was placed in the center of the PDA plate. And then,
119 the strains to be screened were placed on 4 corners 3cm away from the center of the
120 plate and incubated at 28°C for 48h. 24 strains that shrunk the hyphae of the pathogenic
121 bacteria were selected and saved as the re-screening objects. (2) Fine screening: Using
122 the plate confrontation method, the pathogenic bacteria was inoculated in the center of
123 PDA plate, and the re-screening strains were spotted in 3 positions 2.5cm away the
124 pathogenic bacteria cake with a sterile inoculation loop to inoculate only the peach
125 brown rot fungus. Three replicates plates was incubated at 28°C for 7days to observe
126 the antibacterial effect. And representative single colony that had highest antagonistic
127 was selected and kept at 4°C to be tested.

128 The 16S rDNA extracted from the strain with highest antagonistic effect on peach
129 brown rot, as a PCR template, was amplified and sequenced using the universal primers
130 27F (5' -AGTTTGATCMTGGCTCAG-3') and 1492R (5' -GGTACCTTGTTACGACTT-3')
131 according to previous study(Galkiewicz and Kellogg 2008). Nucleotide sequence was
132 compared in GenBank database (Nucleotide Blast) using the BLAST search tool to
133 accurately identify the bacterium(Tan et al. 2020). Meanwhile the Neighbor-joining
134 method was selected to construct sequencing results of biocontrol strain into a
135 Phylogenetic tree through MEGA 7.0 software.

136 ***2.2 Cell growth curves under Cd stress***

137 The pure cultured strain LYX-1 at logarithmic growth phase ($OD_{600}=1.5 \pm 0.2$)
138 were seeded in LB medium containing different Cd^{2+} concentrations(0, 5, 10, 20, 50,
139 100 mg/L) at 2% inoculation amount, meanwhile, conical flasks were incubated at 30°C
140 with 150 rpm on a shaker. The OD_{600} values were monitored at different time intervals
141 using ultraviolet spectrophotometer (Shimadzu UV-2450, Japan) to construct growth
142 curves. The Cd ion stock solution used in the above experiment was prepared in 1000
143 mL volumetric flask by dissolving 2.74g $Cd(NO_3)_2 \cdot 4H_2O$ (analytical grade) purchased
144 from Sinopharm Chemical Reagent Co., Ltd (Shanghai, PRC) in deionized water
145 (Millipore, 18.2Ω).

146 ***2.3 Sorbents preparation***

147 The pure cultured strain LYX-1 was seeded in 600 mL sterile LB medium in 1000
148 mL flasks at 1% inoculation amount and cultured for 48 h at 30°C, 150 rpm on a
149 constant temperature shaker. Living cell adsorbent was prepared by centrifuging the
150 bacterium suspension at 4°C, 8000 rpm for 10 min, while dead cell adsorbent was
151 harvested by centrifuging the bacterial suspension that has been sterilized at 121°C for
152 30 min. Both living and dead pellet were washed 3 times and re-suspended with sterile
153 water, then biomass was stored in a 4°C refrigerator until use. The concentration (grams
154 per liter) of above cell suspension was tested by drying an aliquot to constant weight at
155 80°C (Huang et al. 2013, Xu et al. 2020).

156 ***2.4 Biosorption Cd^{2+} experiments by strain LYX-1***

157 ***2.4.1 pH effects***

158 The initial solution pH values for sorption experiment were adjusted using 1 M
159 NaOH and 1 M HNO_3 . Sorption experiments were conducted in 50 mL centrifuge tubes
160 containing 20 mL Cd^{2+} aqueous solution, 1.0 g/L living and dead sorbents, which were
161 agitated at a speed of 180 rpm for 6 h. The metal solutions used for the sorption
162 experiments were diluted from 1000ppm (metal concentration) $Cd(NO_3)_2$ stock
163 solution. All experiments were performed at ambient conditions and in triplicate. The
164 sorbents was removed by centrifugation at 10000rpm for 10min and the supernatant
165 filtrated through 0.22 μm filter (PVDF, Sterile) was used to measured remaining Cd^{2+}
166 via ICP-MS (Perkin Elmer 600X, USA). The pH was measured by pH meter (PHS-25,

167 INESA, China)(Xu et al. 2020).

168 **2.4.2 Biosorbent dosage effects**

169 To examine the effects of the biosorbent dosage, the biosorption experiments were
170 carried out at different dosage(0.2-3.0g/L). The experiments were performed at optimal
171 pH 8, 30°C, 180rpm and 50mg/L Cd²⁺ for 6h. All experiments were performed at
172 ambient conditions and in triplicate.

173 **2.4.3 Contact time effects and sorption kinetic characteristics**

174 The optimal pH(8.0) and biomass(1.0g/L) was mixed with different contact time
175 (0-300min) at 50 mg/L Cd²⁺. All experiments were performed at 30°C, 180rpm for 6h
176 and in triplicate. To determine the rate-limiting steps by of Cd²⁺ biosorption by the
177 strain LYX-1, Pseudo-first and pseudo-second order rate equation were used to fit the
178 kinetic experimental data to study the biosorption mechanism.

179 Pseudo-first order kinetic model has long been widely applied(Ho 2006), The form is:

$$180 \ln(q_e - q_t) = \ln q_e - k_1 t \quad (1)$$

181 Where q_e and q_t are the amounts of the Cd²⁺ sorbed at equilibrium and at any
182 time t (mg/g), k_1 is the pseudo-first order rate constant of sorption (1/min).

183 The pseudo-second order kinetic equation(Ho and McKay 1999) is shown below:

$$184 \frac{t}{q_t} = \frac{1}{k_2 q_e^2} + \frac{t}{q_e} \quad (2)$$

185 Where k_2 is the pseudo-second order rate constant, g/ (mg min), respectively, q_e
186 and q_t (mg/g) were defined elsewhere.

187 **2.4.4 Initial Cd²⁺ concentrations and sorption isotherm experiments**

188 The optimal pH(8.0) and biomass(1.0g/L) was mixed with different concentrations
189 of Cd²⁺ (0-50mg/L). All experiments were performed at 30°C and 180rpm in triplicate.
190 Langmuir and Freundlich isotherm equations were frequently used to analyze
191 equilibrium data in related research (Masoudzadeh et al. 2011, Ozturk 2007, Zhou et al.
192 2018). The Cd biosorptive performance of the strain LYX-1 was simulated by using
193 Langmuir and Freundlich isotherm equations, as follows(Freundlich 1906, Langmuir
194 1918)

195 Langmuir equation: $q_e = \frac{q_{\max} K_L C_e}{1 + K_L C_e}$ (3)

196 Freundlich equation: $q_e = K_f C_e^{\frac{1}{n}}$ (4)

197 Where q_e is the amount of Cd sorbed at equilibrium (mg/g), C_e is the Cd
 198 equilibrium concentration (mg/L), q_{\max} is saturated sorption capacity of aqueous
 199 solution for Cd^{2+} and K_L is a Langmuir constant related to the sorption strength. Here
 200 K_f is Freundlich coefficient indicating sorption capacity, n , a constant related to Cd ion
 201 concentration, characterizes adsorption intensity, respectively, q_e and C_e were described
 202 earlier.

203 Another dimensionless constant separation factor R_L of Langmuir isotherm model can
 204 be expressed as following:

205 $R_L = \frac{1}{1 + K_L C_0}$ (5)

206 Where C_0 is the highest Cd^{2+} concentration (mg/L), K_L is a Langmuir constant, R_L
 207 reflects the nature of biosorption process ($R_L > 1$: unfavorable; $R_L = 1$: linear; $0 < R_L < 1$:
 208 favorable; $R_L = 0$: irreversible).

209 The Dubinin-Radushkevich (D-R) was selected to study the nature of the sorption
 210 phenomena either physical or chemical sorption, govern the characteristic of not
 211 assuming a homogeneous surface or constant adsorption potential (Dubey and Gupta
 212 2005, Zhou et al. 2018). It can be expressed as:

213 $\ln q_e = \ln q_{\max} - \beta \varepsilon^2$ (6)

214 Where q_e (mg/g) and q_{\max} (mg/g) are described above, β (mol^2/kJ^2) is the parameter
 215 with respect to the mean free energy of sorption per molecule of the adsorbate, ε (kJ/mol)
 216 is the adsorption potential, and the mean free energy E (kJ/mol) can be computed using
 217 following formula (Kaur et al. 2015):

218 $E = \frac{1}{\sqrt{2\beta}}$ (7)

219 For the adsorption from aqueous solution, the adsorption potential can be defined
 220 as (Hu and Zhang 2019):

221 $\varepsilon = RT \ln(1 + 1/C_e)$ (8)

222 **2.5 PCR amplification of Cd-resistant genes**

223 According to the current research on the mechanism of strain resistance to Cd, its
224 resistance was mainly controlled by universal cadA and Czc systems(Ayangbenro et al.
225 2019, NIES et al. 1898, Wei et al. 2009). We could screen for the resistance genes to
226 further explore the mechanism of reducing or eliminating heavy metal toxicity by
227 biocontrol *Paenibacillus* sp., LYX-1 through PCR amplification of Cd²⁺-related
228 genomes (cadA, CzcA, CzcB and CzcD). The genomic DNA of strain LYX-1. used as
229 a template, amplified as follows: pre-denaturation at 98°C for 3 min; 35 cycles of
230 denaturation at 98°C for 10s, annealing at X°C for 10s, extension at 72°C for 15 s;
231 followed by a final extension step at 72°C for 3 min. The primer sequences selected
232 with reference to the previous studies of the above-mentioned enzyme genes were listed
233 in **Table S1**. All primers used for PCR were synthesized by Tsingke biotechnology Co.,
234 Ltd. (Beijing, China).

235 ***2.6 Characterization to biosorption mechanisms of Cd²⁺ by strain LYX-1***

236 Samples of living and dead cells before and after 50 mg/LCd²⁺ biosorption were
237 collected and freeze-dried for the following tests. Cells were immobilized in
238 glutaraldehyde at 4°C overnight and then washed using phosphate buffer (pH 7.2) for 3
239 times. The washed biomass was finally dehydrated in alcohol, and followed by
240 immobilization and being cut into 70-90 nm thin sheets for transmission electron
241 microscopy (H-7650, Japan), scanning electron microscope coupled with energy
242 dispersive spectroscopy (Nova Nano 450, USA) analysis. Freeze-dried biomass were
243 prepared for Fourier Transform Infrared Spectrometry (Thermo Scientific Nicolet iN10,
244 USA) and X-ray photo-electron spectroscopy (Thermo Scientific K-Alpha, USA) to
245 study the fundamental properties and underlying encapsulation mechanisms of
246 adsorbents before and after biosorption according to previous methods(Huang et al.
247 2020).

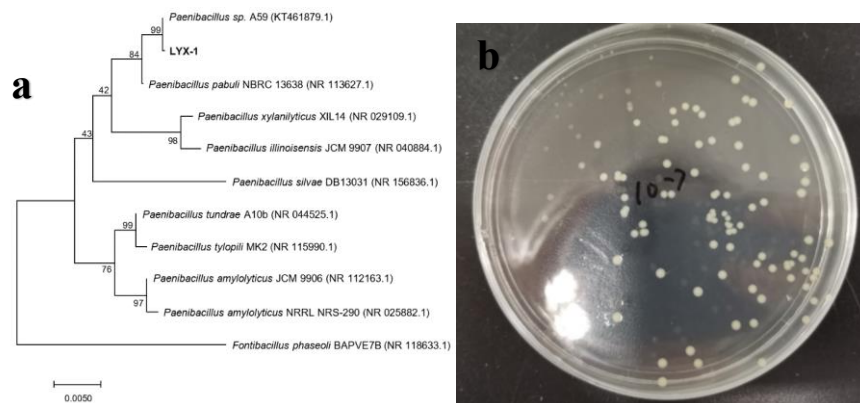
248 ***2.7 Statistical analysis***

249 All experiments were performed in triplicates. Statistical analysis was carried out
250 using SPSS 20.0 software. All drawing and model fittings were generated using Origin
251 2018 software. The phylogenetic tree was constructed by MEGA 7.0.

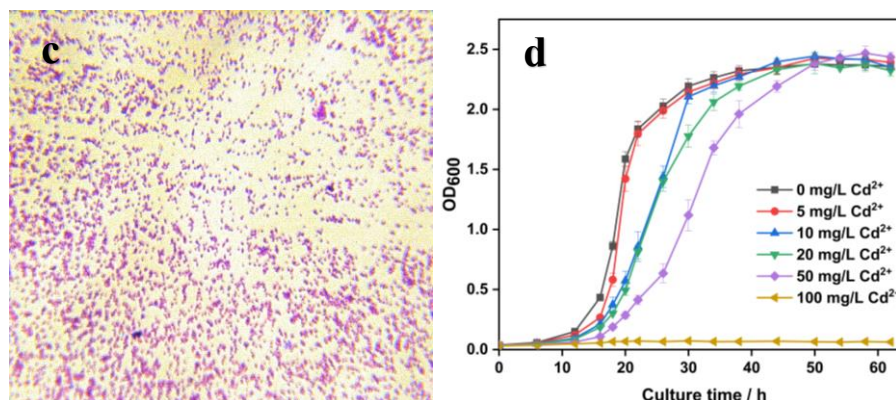
252 3. Results and discussion

253 3.1 The isolation and identification of biocontrol strain *Paenibacillus* sp. LYX-1

254 Biocontrol strain *Paenibacillus* sp. LYX-1 with antagonistic to peach brown rot
255 was isolated from rhizosphere soil in peach orchard in Fenghua city, Zhejiang province,
256 China. The significant antagonism to peach brown rot could be seen in plate antagonism
257 test from **Fig. S1**. The 16S rDNA sequences of LYX-1 aligned with the published
258 sequences in NCBI database using BLAST (<https://www.ncbi.nlm.nih.gov>) had the
259 highest similarity (99.62%) with *Paenibacillus* sp.. The phylogenetic tree constructed
260 also indicated that the strain had 99% threshold with *Paenibacillus* sp. (**Fig. 1a**). Thus,
261 it was named *Paenibacillus* sp.. The strain LYX-1 and its GenBank accession number
262 was MZ234160. The strain LYX-1 has also been deposited in China General
263 Microbiological Culture Collection Center (CGMCC accession No. 22158) as a patent
264 strain. The strain on LB medium was round, light yellow with smooth edges(**Fig. 1b**).
265 **Fig. 1c** proved that strain LYX-1 was Gram-positive. Biocontrol strain *Paenibacillus*
266 sp. LYX-1 was also identified with higher Cd²⁺ resistance(**Fig. 1d**).



267



268

269

Fig. 1. (a) the neighbor-joining tree based on 16S rDNA gene sequences, showing the phylogenetic relationships

270 between strain LYX-1 with other strains, (b) the colony morphology, (c) gram staining characteristics and (d)
271 growth curves in presence of different initial Cd²⁺ concentrations of the *Paenibacillus* sp. strain LYX-1.

272 **3.2 Effects of Cd²⁺ concentrations on growth curves of *Paenibacillus* sp. LYX-1**

273 Microbial growth was influenced directly by the microbial activity under different
274 concentrations of heavy metal(Huang et al. 2014, Sun et al. 2020, Tan et al. 2020). As
275 shown in **Fig. 1d**, the growth of *Paenibacillus* sp. LYX-1 was barely affected and the
276 maximum OD₆₀₀ value even exceeded 2.4 under 20 mg/L Cd²⁺. As the concentration
277 increased, the logarithmic growth stage had obvious delays, which might due to stressed
278 metabolic pathway and internal biochemical reactions(Sun et al. 2020). Increasing the
279 Cd²⁺ concentrations did not significantly decreased the strain LYX-1 activity (**Fig. 2**),
280 suggesting that the stain LYX-1 had a good environmental adaptability that could
281 continue to grow in the presence of 50 mg/L Cd²⁺. And, the stain could not grow when
282 Cd²⁺ reached 100 mg/L. In sum, the strain LYX-1 had high Cd resistance (50mg/L).

283 **3.3 Impact factors optimization to Cd²⁺ adsorption by *Paenibacillus* sp. LYX-1**

284 The Cd²⁺ biosorption performance of living and dead biomass was complex, and
285 the removal efficiency of Cd²⁺ was closely related to pH, initial Cd²⁺ concentrations,
286 doses and contact time(Yu and Fein 2017, Zhou et al. 2014). To investigate the sorption
287 conditions of living and dead sorbents, effects of these four independent variables were
288 illustrated.

289 **3.3.1 Effects of different pH**

290 Earlier studies have shown that pH was an important factor affecting biosorption
291 process, because it could directly influence the solubility of metal ions, ionization state
292 of functional groups on the microorganism surface(Altowayti et al. 2019, Şahin and
293 Öztürk 2005). As the initial pH increased, Cd²⁺ removal showed a rising tendency (**Fig.**
294 **2a**). Due to the competitive adsorption between hydrogen ions and adsorbed Cd²⁺
295 ions(Zeng et al. 2021), the equilibrium adsorption capacity of heavy metal was just 7.95
296 mg/g and 6.48 mg/g for living and dead cells at the pH 3.0. When the pH reached 4.0,
297 more charged functional groups on the cell surface, such as carboxyl, amino, and
298 hydroxyl began to expose, which strengthened the binding of Cd²⁺ to the adsorption
299 site, thereby increasing the amount of adsorption((Li et al. 2018, Özdemir et al. 2009).

300 Meanwhile, as the solution pH increased, more Cd^{2+} would be fixed on to the
301 negatively-charged cell surface due to the electrostatic adsorption. Notably, the
302 presence of a highest point between pH 3 and 8, the optimum pH value for sorption was
303 determined at 8.0 for both living cells and dead cells, which suggested that the LYX-1
304 had an excellent pH buffering performance. It was calculated that when pH=8.0, heavy
305 metal ions not reached the precipitation equilibrium constant, so hydroxide
306 precipitation not generated in the solution.

307 **3.3.2 Effects of initial Cd^{2+} concentrations**

308 **Fig. 2b** showed the adsorption capacity of *Paenibacillus* sp. at different Cd^{2+}
309 concentrations ranging from 0 to 50 mg/L. In general, with the increase of the initial
310 concentrations of Cd ions, the biosorption capacity gradually increased for both living
311 and dead cells, which implied that an increase in the initial Cd^{2+} concentration generated
312 a driving force and reduced the mass transfer resistance between Cd ions and
313 sorbents(Masoudzadeh et al. 2011). Owing to the limited biosorption sites of
314 sorbents(Xu et al. 2020), the sorption capacity reached saturation in higher
315 concentration treatment (more than 30 mg/L). In addition to the adsorption of living
316 cells, there was also intracellular accumulation(Li et al. 2010). Herein, the adsorption
317 capacity of living cells(18.019 mg/g) was slightly higher than dead cells (14.847 mg/g)
318 when Cd^{2+} concentration was 20 mg/L. Note that, the removal capacities of living and
319 dead cells were as high as 90.39% and 75.67% under the 20 mg/L Cd^{2+} , respectively.
320 Thus, the *Paenibacillus* sp., a promising and highly efficient biocontrol biosorbent,
321 could be applied for heavy metal sewage treatment.

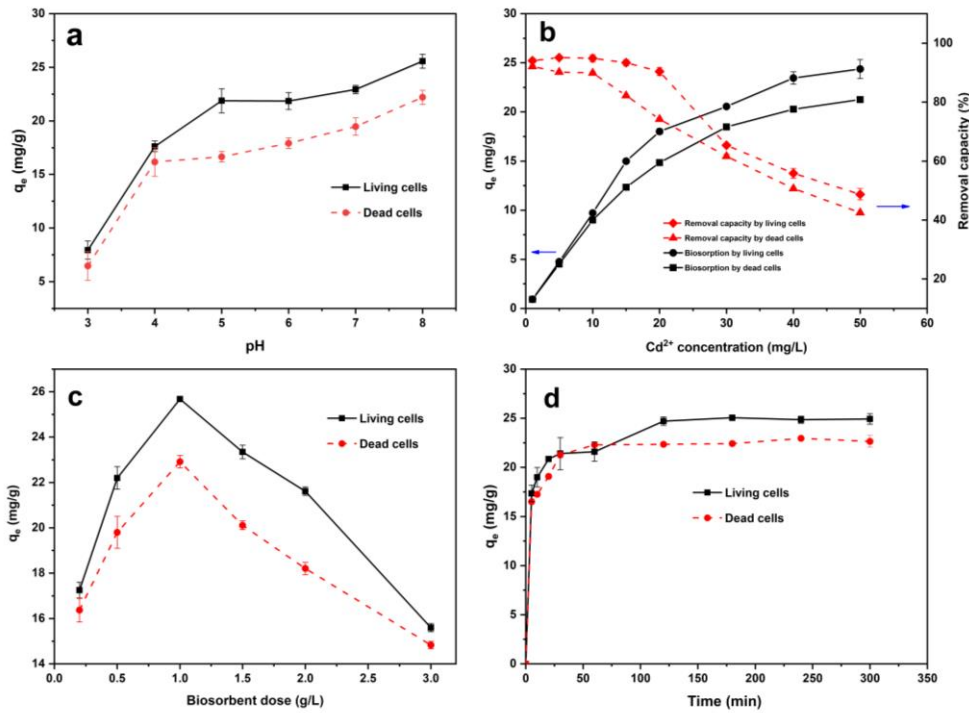
322 **3.3.3 Effects of adsorbent dose**

323 The variation of equilibrium uptake for Cd ions at different biosorbent dose for
324 each living biomass and dead biomass were shown in **Fig. 2c**, which indicated that Cd^{2+}
325 was adsorbed by the living biomass more strongly than dead biomass and two
326 adsorbents had similar patterns for Cd removal. The adsorption capacity increased
327 gradually as the biomass dose increased from 0.2 to 1.0 g/L, which could be explained
328 that more binding sites were available and thus the biosorption capacity went up with
329 the increase of dose(Sun et al. 2011). However, the biomass of strain LYX-1 presented

330 a decline trend with an increased biosorbent dose from 1.0g/L to 3.0 g/L. It has been
331 reported that biosorbent generated aggregation under high biosorbent concentrations,
332 causing the decrease in effective contact area between cells and metal ions(Zhu et al.
333 2016). Therefore, the optimum living and dead cells dosage of all following
334 experiments was selected as 1.0 g/L. Therefore, it was obvious that redundant
335 adsorbents were not necessary for an efficient biosorption performance under specific
336 initial concentration.

337 **3.3.4 Effects of contact time**

338 As reported by Sun(Sun et al. 2011), contact time had a significant effect on the
339 equilibrium biosorption. Cd²⁺ biosorption by *Paenibacillus* sp. LYX-1 under different
340 contact time (0-300 min) at 50 mg/L initial Cd²⁺, pH 8.0, 30°C and 180 rpm were
341 studied. The effect of contact time on the amount biosorbed was presented in **Fig. 2d**.
342 For Cd²⁺, saturation levels of living and dead biomass were obtained after 120 min and
343 60 min, respectively, which indicated that LYX-1 had a higher adsorption efficiency.
344 The biosorption capacity of the two adsorbents for Cd increased with the extension of
345 time. It showed a fast adsorption process within 30 minutes and a slow adsorption
346 process within 30-60 minutes for dead biosorbent. This was because the adsorption sites
347 on the bacterial surface gradually reached saturation. After reaching 60 and 120 minutes,
348 the adsorption curve showed a relatively gentle trend, indicating that the adsorbent and
349 adsorbate reached adsorption equilibrium. It was also noticeable that the experimental
350 results were consistent with previous studies on the biosorption of Cd ions (Li et al.
351 2010, Xu et al. 2020). The shaking time was determined to be 3 h for the rest of the
352 batch experiments to make sure the equilibrium was reached.

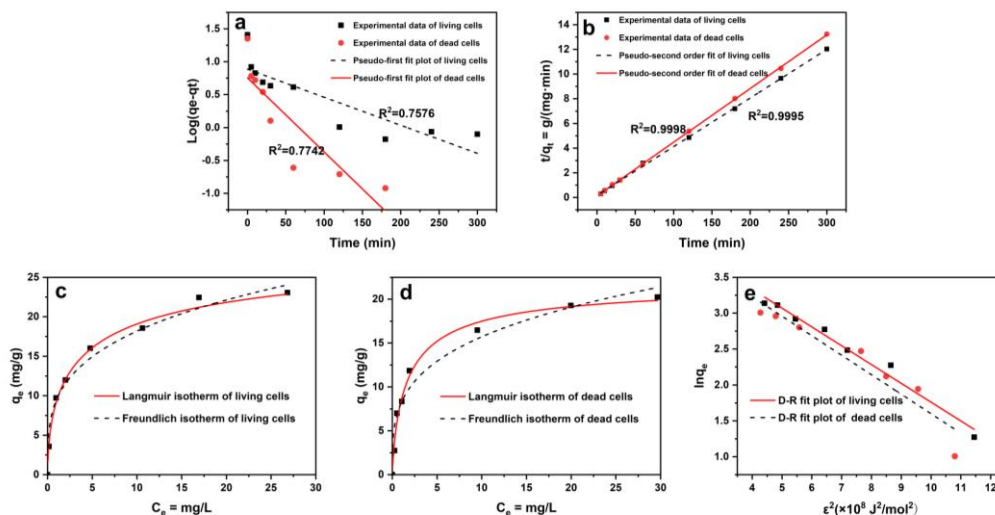


353

354 **Fig. 2.** Effects of environmental factor on Cd²⁺ biosorption by living and dead biocontrol strain LYX-1 (a) pH (b)
 355 initial Cd²⁺ concentrations (c) biosorbent dose (d) contact time.

356 **3.4 Adsorption kinetic characteristics**

357 According to formulas (1) and (2), the experimental data was fitted to obtain the
 358 kinetic fitting diagrams. As depicted in **Fig. 3a** and **3b**, clearly, the effect of the pseudo-
 359 second-order rate equation was better than pseudo-first-order rate equation, which
 360 suggested that the influence of the mass diffusion step on the adsorption rate could be
 361 negligible and rate-limiting step was a chemical adsorption process (Ho 2006, Ho and
 362 McKay 1999). This result was consistent with numerous reports on the (Abdolali et al.
 363 2016, Feng et al. 2011, Xu et al. 2020). The equilibrium adsorption capacity of ions
 364 calculated by the pseudo-second-order rate equation was basically consistent with the
 365 measured value (**Table 1**). Thus, the pseudo-second-order kinetic parameters could be
 366 used to calculate the equilibrium adsorption capacity and removal rate.



367

368 **Fig. 3.** The linear form of (a) Pseudo-first and (b) Pseudo-second order model for Cd^{2+} adsorption onto living and
 369 dead cells; biosorption isotherm images of Langmuir (q_{max} : mg/g, b: L/mg), Freundlich (K_F , n_f ($0.1 < 1/n_f < 1$)) for (c)
 370 Cd^{2+} biosorption onto living cells, (d) Cd^{2+} biosorption onto dead cells and Dubinin-Radushkevich (D-R) for (e)
 371 Cd^{2+} biosorption onto both living and dead cells.

372

373 **Table 1** Kinetic parameters obtained for the adsorption of Cd^{2+} using the linear method and isothermal constants,
 374 coefficient of determination (R^2) for the models fitted to equilibrium Cd^{2+} biosorption onto biomass *Paenibacillus*
 375 sp. LYX-1 strain (data calculated by equation of regression line obtained by software Origin 2018).

Models	Parameters	biosorbents	
		Living biomass	dead biomass
Pseudo-first order kinetic	$q_{e, \text{exp}}$ (mg/g)	23.2854	23.2854
	$q_{e, \text{cal}}$ (mg/g)	7.7250	5.7030
	k_1 (min^{-1})	9.8338×10^{-3}	2.5930×10^{-2}
	R^2	0.7273	0.7365
Pseudo-second order kinetic	$q_{e, \text{exp}}$ (mg/g)	23.7158	20.5453
	$q_{e, \text{cal}}$ (mg/g)	23.3614	19.9568
	k_2 (mg/g min)	8.5471×10^{-3}	1.5590×10^{-2}
	R^2	0.9894	0.9798
Langmuir	q_{max} (mg/g)	30.6790	24.3752
	K_L (L/g)	0.4130	0.6244
	R_L	0.0461	0.0310
	R^2	0.9704	0.9871
Freundlich	K_F (mg/g)	9.4936	8.2306
	n	3.48831	4.5157
	R^2	0.9915	0.9378
Dubinin-Redushkevich (D-R)	β (mol^2/kJ)	2.6201×10^{-9}	2.7162×10^{-9}
	E (kJ/mol)	13.8313	13.5676
	R^2	0.9757	0.9065

376

377 3.5 Isothermal adsorption characteristics

378 The adsorption isotherm to some extent reflected the strength of interaction,

379 surface properties and affinity of adsorbent for different heavy metal ions(Mohapatra
380 et al. 2019). In this study, Langmuir, Freundlich and D-R isotherm models were selected
381 to simulate favorable equilibrium uptake curve and reveal the adsorption behavior of
382 living and dead cells *Paenibacillus* sp. LYX-1(**Fig. 3**). In case of Langmuir isotherm
383 equation, the biosorption feature was determined by both q_{\max} and K_L value(Ranjan et
384 al. 2009). As shown in **Fig. 3c** and **table 1**, the regression coefficient R^2 of Langmuir
385 and Freundlich equations were 0.9704 and 0.9915, respectively, indicating that these
386 two models could describe the adsorption process of living biomass well. This result
387 suggested that Cd^{2+} biosorption by living adsorbent was more likely to be monolayer
388 and heterogenous surface adsorption, besides, other intracellular accumulation
389 mechanisms might be involved in removal process of Cd^{2+} by living cells. In addition,
390 the Langmuir model ($R^2=0.9871$) was more applicable to simulate the dead cell
391 adsorption process than Freundlich ($R^2=0.9478$), indicating that the nature of
392 biosorption by dead cells was a monolayer and non-heterogenous adsorption. As seen
393 in **table 1**, the maximum adsorption capacity of living and dead cells for Cd sorption,
394 estimated from the Langmuir q_{\max} parameter, was found to be 30.6790 mg/g and
395 24.3752 mg/g. The comparison of R_L for living biomass ($R_L=0.0461$) and dead biomass
396 ($R_L=0.0310$) showed that living cells had a higher adsorption capacity. The high
397 adsorption properties of *Paenibacillus* sp. meant that it had a strong fixation ability to
398 Cd and might reduce the bioavailability of Cd^{2+} in the contaminated soil. Therefore, the
399 biocontrol LYX-1 might control the migration of heavy metal pollutants into plants
400 while exerting its biocontrol effect on pathogenic bacterium.

401 For D-R model, the plots of $\ln q_e$ versus ε^2 were shown in **Fig. 3e**, and parameters
402 were presented in **Table 1**. Additionally, the magnitude of E might give useful
403 information about the type of adsorption process (physical or chemical)(Ishola et al.
404 2014, Tran et al. 2016). Physical adsorption arises from relatively weak interactions
405 such as van der waals force, while chemical adsorption involves stronger chemical
406 interactions (chemical bonding) with attendant transfer of electrons between the
407 adsorbent and adsorbate(Tran et al. 2017). In essence, the value of E for living and dead
408 biomass were found to be with the range from 8 kJ/mol to 16 kJ/mol, indicating that

409 chemisorption (ion exchange complexation and precipitation) controlled the adsorption
410 process.

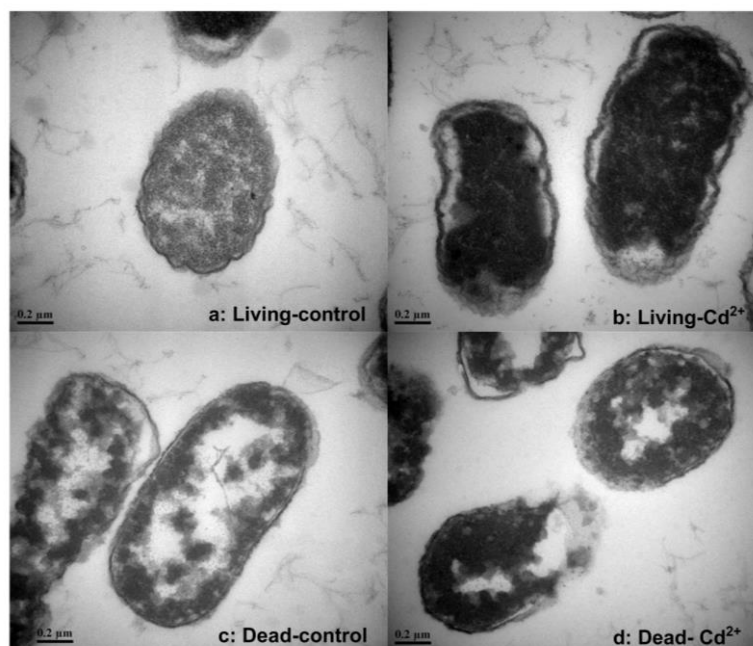
411 **3.6 Mechanisms of Cd²⁺ resistance and biosorption by strain LYX-1**

412 **3.6.1 Amplification of Cd-resistant genes**

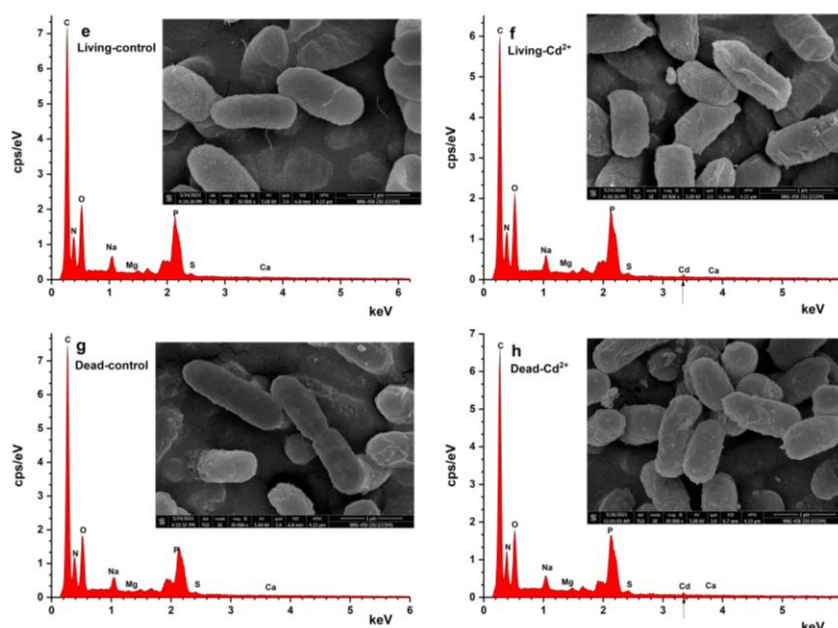
413 *Paenibacillus* sp. LYX-1 resistant to Cd²⁺ was chosen for sequence analysis of the
414 cadA, CzcA, CzcB, CzcD, which had the potential to reduce or eliminate heavy metal
415 Cd²⁺ toxicity(Wei et al. 2009). **Fig. S2** showed that *Paenibacillus* sp. LYX-1 processed
416 Cd²⁺-resistant genes (CzcD) that could modify the protein, determine the specificity to
417 the metal substrate, and realized the resistance to Cd through efflux system(Legatzki et
418 al. 2003). The detection of CzcD demonstrated that *Paenibacillus* sp. had ability to
419 resist 50 mg/L Cd²⁺ (**Fig. 2**). Besides, the function of efflux CzcD gene further
420 explained the insignificant difference in the maximum adsorption capacity of living
421 (30.6790mg/g) and dead biosorbent (24.3752mg/g) in **Table 1**.

422 **3.6.2 TEM analysis**

423 In order to study the intracellular accumulation and extracellular adsorption of
424 Cd²⁺ by biocontrol strain LYX-1, TEM was used to observe the changes of bacterial
425 surface morphology in the presence of Cd²⁺. It could be seen from the **Fig. 4a** that the
426 living control cells were full of intracellular and had uniform cytoplasm, complete cell
427 wall structure, clear boundaries. On the one hand, when under the stress of 50 mg/L
428 Cd²⁺, living biomass had a clear gap between the cell wall and cytoplasm of living
429 biomass with high-density black particulate matter appearing inside and outside the cell
430 (**Fig. 4b**). This might be attributed to the contraction of the cytoplasm to increase the
431 intracellular accumulation of Cd²⁺ and form a resistance mechanism(Sun et al. 2020).
432 Additionally, this also verified the results of the previous isotherm and kinetic
433 experiments that not only fast surface adsorption occurred in living cells, but also
434 relatively slow intracellular accumulation (**Fig. 3**). After the high temperature heat
435 treatment, the cytoplasm of dead cells severely shrank and appeared different size
436 vacuoles (**Fig. 4c**), besides, **Fig. 4d** appeared high-density black particulate matter,
437 indicating that the adsorption of Cd by dead cells was mainly concentrated on the outer
438 edge and periplasmic space, which was consistent with Huang et al. (Huang et al. 2013).



439



440

441 **Fig. 4.** Submicroscopic structures of *Paenibacillus* sp., LYX-1 (a) nature living cells, (b) 50 mg/L Cd²⁺-loaded
 442 living cells, (c) dead cells, (d) 50 mg/L Cd²⁺-loaded dead cells; scanning electron micrograph (SEM) and energy
 443 dispersive spectrometer (EDS) of the (e) living cells without Cd²⁺ treatment; (f) living cells treated with 50 mg/L
 444 Cd²⁺, (g) dead cells without Cd²⁺ treatment, (h) dead cells treated with 50 mg/L Cd²⁺.

445 3.6.3 SEM-EDS analysis

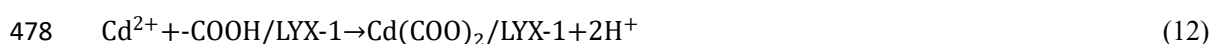
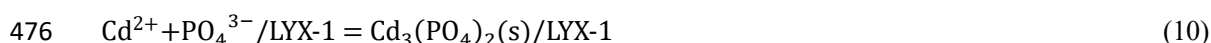
446 Based on the micro-characterization SEM-EDS study of biomass, Cd removal
 447 mechanism by the strain *Paenibacillus* sp. was further analyzed. **Fig. 4(e)-(h)** showed
 448 surface characteristic changes of living and dead cells morphology before and after
 449 Cd²⁺ removal. We found that the surface of living cells appeared smooth and short-rod

450 shapes, while living cells after absorbing Cd²⁺ became rough and ruptured,
 451 accompanied by a large amount of flocculent sedimentation (**Fig. 4e and f**). Compared
 452 with living cells, dead cells seemed to be rougher, which might be caused by
 453 temperature heat treatment. After the biosorption of Cd, precipitated materials appeared
 454 on the surface of dead cells, indicating that numerous Cd²⁺ ions were adsorbed on the
 455 surface of dead biomass. The EDS analysis further verified the adsorption of Cd²⁺ by
 456 the biosorbents. No Cd peaks were detected in pristine cells. However, the peaks of
 457 Cd²⁺ with all the other elements was detected in the EDS analysis of two biomass
 458 samples after Cd biosorption. Elemental variation of strain LYX-1 before and after
 459 biosorption was in **Table S2**. Presence of Cd on cell surface after adsorption as seen
 460 from EDS images (**Fig. 4g and 4h**) proved the biosorption of Cd²⁺ by living and dead
 461 biosorbents of *Paenibacillus* sp..

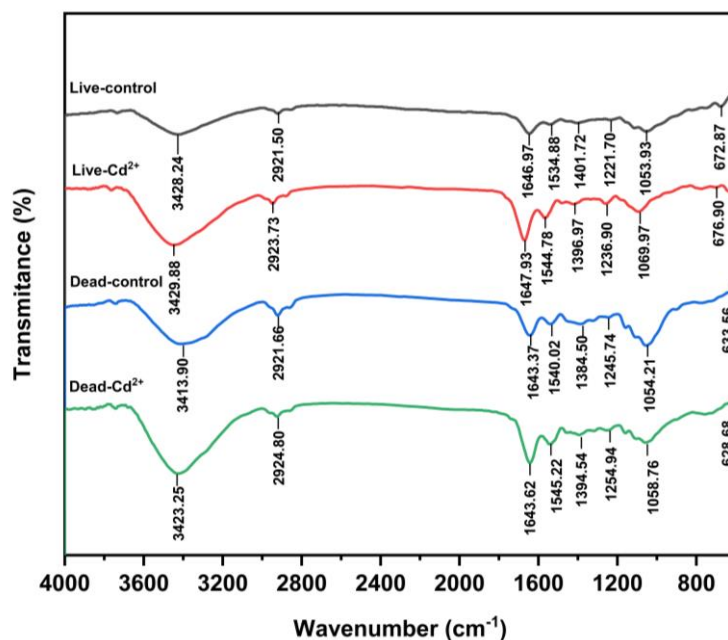
462 **3.6.4 FTIR analysis**

463 In order to confirm the changes of functional groups involved in the Cd binding
 464 of biomass, the FTIR analysis was carried out. The FTIR spectrum of raw and Cd²⁺-
 465 loaded living and dead biosorbent were presented in **Fig. 5**, where characteristic
 466 transmittance peaks listed in were identified according to previous reports (Chen et al.
 467 2012, Huang et al. 2016, Sun et al. 2020).

468 For untreated living and dead cells, in **Table S3**, the peaks observed at 3429.88,
 469 2923.73, 1647.93, 1544.78, 1236.90, 1069.97, 672.87 (living) and 3413.90, 2921.66,
 470 1643.37, 1540.02, 1245.74, 1054.21 and 633.56 (dead) were assigned to associated O-
 471 H, N-H., -CH₂, amide I (-C=O/C-N), amide II (C-N/N-H), S²⁻, C-N and phosphate, or
 472 sulfate functional groups, respectively(Peng et al. 2020). The free Cd²⁺ could be fixed
 473 by the abundant oxygen-containing and amino functional groups via the formation of
 474 surface complexation, which could be described:



480 After Cd^{2+} biosorption, there was only slight shift of groups between control and
 481 Cd^{2+} treated groups. However, attributed to interaction between adsorbents and heavy
 482 metal, -OH, -NH, -CH₂, -C=O, O=C-O, C-N, S²⁻ and phosphate functional groups were
 483 red or blue shifted when compared to nature living and dead cells, suggesting that those
 484 shifted bonds and correspond functional groups might be involved in Cd
 485 biosorption(Xu et al. 2020).

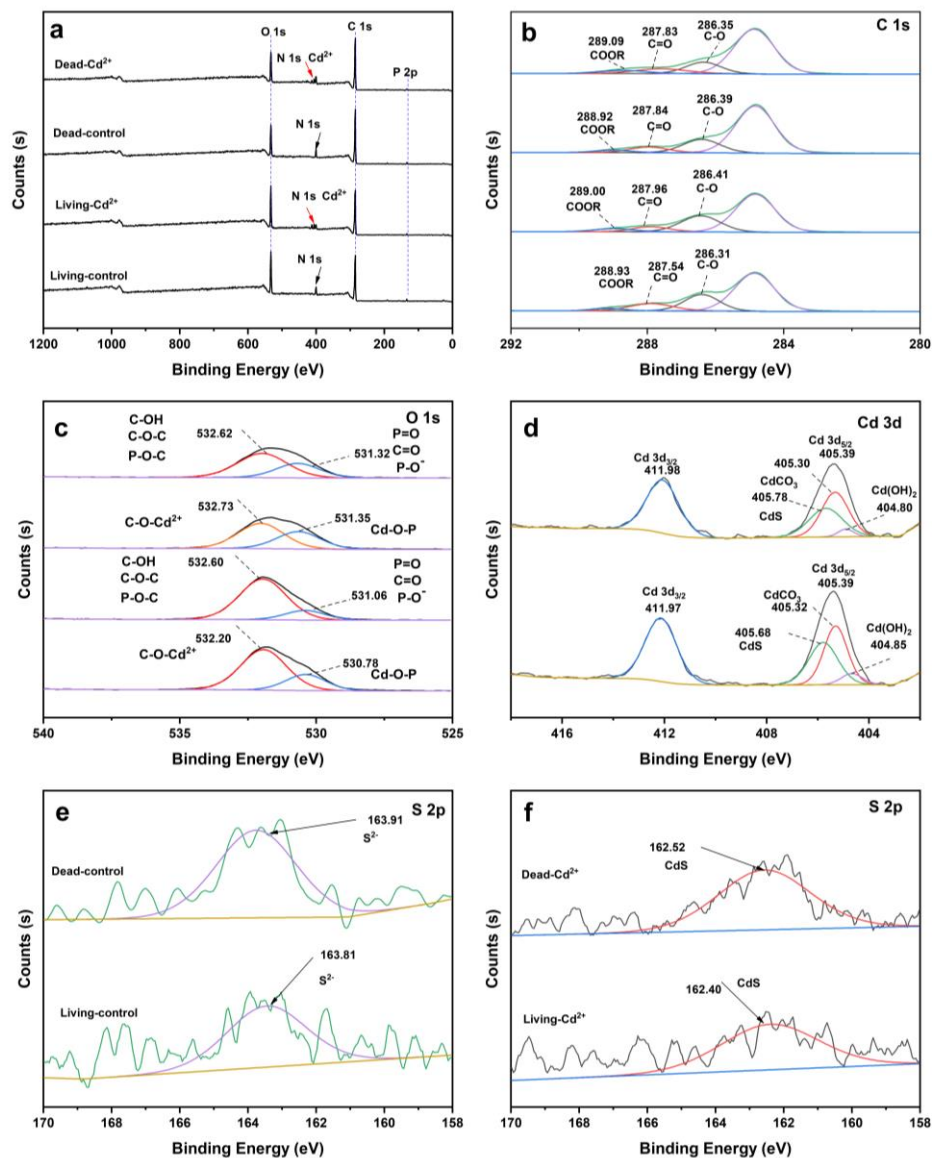


486
 487 Fig. 5. FTIR spectra of the living and dead cell before and after adsorption of Cd^{2+} .

488 3.6.5 XPS analysis

489 Full-range XPS spectra of *Paenibacillus* sp. before and after biosorption were
 490 shown on Fig. 6a, which proved Cd^{2+} were adsorbed onto the strain LYX-1. The peaks
 491 of C-O at 286.31eV and 286.39eV (BE) of living and dead cells, respectively, were
 492 slightly reduced (Fig. 6b), which indicated that surface reducing groups such as C-OH
 493 could form precipitation with Cd^{2+} or provide protons to promote the formation of CO-
 494 Me (CO- Cd^{2+})(Ho et al. 2017). By comparing the O 1s spectra of the control and
 495 experimental groups, the peaks of O 1s at 532.60eV and 532.62eV of living and dead
 496 cells were also considered as C-O- Cd^{2+} (Fig. 6c). Peaks of Cd detected after the
 497 adsorption could be divided into peaks at 405.39eV and 411.98eV, corresponding to Cd
 498 3d_{5/2} and Cd 3d_{3/2} (Fig. 6d), respectively. There peaks (404.85eV, 405.30 eV, 405.78 eV
 499 for living cells, 404.80 eV, 405.30 eV and 405.78 eV for dead cells) could be possibly

500 ascribed to $\text{Cd}(\text{OH})_2$, CdCO_3 , and CdS . **Fig. 6e** and **Fig. 6f** also demonstrated the
 501 generation of CdS precipitation. XPS results also identified that Chemisorption
 502 controlled the biosorption process of Cd^{2+} by LYX-1 (**Fig.3e**).



503
 504 **Fig. 6.** XPS spectra of *Paenibacillus* sp. LYX-1 living and dead cells before and after adsorption of Cd^{2+} . (a) Wide
 505 scan, (b) C 1s spectra, (c) O 1s spectra, (d) Cd 3d spectra, (e) S 2p spectra before biosorption, (f) S 2p spectra after
 506 biosorption.

507 4. Conclusions

508 This study successfully isolated and identified a novel biocontrol bacterium with
 509 high-Cd resistance from soil contaminated by HMs, named *Paenibacillus* sp. LYX-1.
 510 PCR amplification showed that LYX-1 had the *CzcD* gene responsible for Cd
 511 detoxification by removing Cd^{2+} from the cytoplasm or periplasmic to extracellular

512 medium. pH, initial Cd²⁺ concentration, adsorbent dose and contact time had significant
513 effects on the Cd capacity of living and dead biomass in batch adsorption test. Pseudo-
514 second order kinetic model was more suitable to two biosorbents. The fitting of
515 Langmuir and Freundlich isotherm showed that there was a monolayer and
516 heterogenous surface process for living cells, while monolayer and non-heterogenous
517 process for dead cells. The E value of two biomasses ranged from 8 kJ/mol to 16 kJ/mol,
518 revealing that chemisorption controlled the adsorption of Cd²⁺ by *Paenibacillus* sp. The
519 maximum capacity obtained were 30.6790 mg/g (living biomass) and 24.3752 mg/g
520 (dead biomass), respectively. TEM, SEM-EDS, FTIR and XPS characterization
521 indicated that extracellular precipitation, ion exchange, and intracellular accumulation
522 might be the main mechanisms for the adsorption of Cd²⁺ by living cells, while there
523 was no intracellular accumulation for dead cells. -OH, -NH, -C=O, O=C-O, C-N, S²⁻
524 and phosphate functional groups participated in the adsorption process of Cd. Therefore,
525 this novel biocontrol *Paenibacillus* sp. can be applied as a promising adsorbent to be
526 used in the simultaneous control of plant rhizosphere diseases and Cd pollution in soil.

527 **Compliance with ethics guidelines**

528 This article does not contain any studies with human or animal subjects performed
529 by either of authors.

530 **Consent for publication**

531 All authors have read the submitted version of the manuscript and agree to submit
532 the work to Environmental Science and Pollution Research, and we all agree that the
533 transfer of copyright from the author to Environmental Science and Pollution Research.

534 **Availability of data and materials**

535 All data generated or analysed during this study are included in this published
536 article and its supplementary information files.

537 **Contributors**

538 Yixin Luo, Min Liao and Xiaomei Xie conceived the idea. Min Liao and Xiaomei
539 Xie designed the research. Yixin Luo, Yuhao Zhang, Na Xu, Xiaomei Xie and Qiyan
540 Fan performed the experiment. Yixin Luo, Min Liao and Xiaomei Xie analysed the data
541 and wrote the manuscript. All authors contributed to the discussion of the manuscript.

542 **Declaration of competing interest**

543 The authors declare that they have no known competing financial interests or
544 personal relationships that could have appeared to influence the work reported in this
545 paper

546 **Acknowledgements**

547 This work was financially funded by the Nation Key Research and Development
548 project of China and the National Natural Science Fund of China (grant number
549 2018YFC1800403, 41571226).

550

551 **References**

- 552 Abdolali, A., Ngo, H.H., Guo, W., Lu, S., Chen, S.S., Nguyen, N.C., Zhang, X., Wang, J. and Wu, Y. (2016) A
553 breakthrough biosorbent in removing heavy metals: Equilibrium, kinetic, thermodynamic and
554 mechanism analyses in a lab-scale study. *Sci. Total Environ.* 542(Pt A), 603-611.
- 555 Abou-Shanab, R.A., van Berkum, P. and Angle, J.S. (2007) Heavy metal resistance and genotypic analysis
556 of metal resistance genes in gram-positive and gram-negative bacteria present in Ni-rich serpentine soil
557 and in the rhizosphere of *Alyssum murale*. *Chemosphere* 68(2), 360-367.
- 558 Ali, M.A., Lou, Y., Hafeez, R., Li, X., Hossain, A., Xie, T., Lin, L., Li, B., Yin, Y., Yan, J. and An, Q. (2020)
559 Functional Analysis and Genome Mining Reveal High Potential of Biocontrol and Plant Growth
560 Promotion in Nodule-Inhabiting Bacteria Within *Paenibacillus polymyxa* Complex. *Front. Microbiol.* 11,
561 618601.
- 562 Altowayti, W.A.H., Algaifi, H.A., Bakar, S.A. and Shahir, S. (2019) The adsorptive removal of As (III) using
563 biomass of arsenic resistant *Bacillus thuringiensis* strain WS3: Characteristics and modelling studies.
564 *Ecotoxicol. Environ. Saf.* 172, 176-185.
- 565 Araujo, R., Dunlap, C. and Franco, C.M.M. (2020) Analogous wheat root rhizosphere microbial
566 successions in field and greenhouse trials in the presence of biocontrol agents *Paenibacillus peoriae* SP9
567 and *Streptomyces fulvissimus* FU14. *Mol. Plant Pathol.* 21(5), 622-635.
- 568 Ayangbenro, A.S., Babalola, O.O. and Aremu, O.S. (2019) Bioflocculant production and heavy metal
569 sorption by metal resistant bacterial isolates from gold mining soil. *Chemosphere* 231, 113-120.

570 Chen, Z., Huang, Z., Cheng, Y., Pan, D., Pan, X., Yu, M., Pan, Z., Lin, Z., Guan, X. and Wu, Z. (2012) Cr(VI)
571 uptake mechanism of *Bacillus cereus*. Chemosphere 87(3), 211-216.

572 Dell'Amico, E., Mazzocchi, M., Cavalca, L., Allievi, L. and Andreoni, V. (2008) Assessment of bacterial
573 community structure in a long-term copper-polluted ex-vineyard soil. Microbiol. Res. 163(6), 671-683.

574 Dubey, S.S. and Gupta, R.K. (2005) Removal behavior of Babool bark (*Acacia nilotica*) for submicro
575 concentrations of Hg²⁺ from aqueous solutions: a radiotracer study. Sep. Purif. Technol. 41(1), 21-28.

576 Feng, N., Guo, X., Liang, S., Zhu, Y. and Liu, J. (2011) Biosorption of heavy metals from aqueous solutions
577 by chemically modified orange peel. J. Hazard. Mater. 185(1), 49-54.

578 Freundlich, H.M.F. (1906) Over the adsorption in solution. J. Chem. Phys. 57, 385-470.

579 Galkiewicz, J.P. and Kellogg, C.A. (2008) Cross-Kingdom Amplification Using Bacteria-Specific Primers:
580 Complications for Studies of Coral Microbial Ecology. Appl. Environ. Microbiol. 74(24), 7828-7831.

581 Han, H., Wang, Q., He, L.Y. and Sheng, X.F. (2018) Increased biomass and reduced rapeseed Cd
582 accumulation of oilseed rape in the presence of Cd-immobilizing and polyamine-producing bacteria. J.
583 Hazard. Mater. 353, 280-289.

584 Hao, Z., Van Tuinen, D., Wipf, D., Fayolle, L., Chataignier, O., Li, X., Chen, B., Gianinazzi, S., Gianinazzi-
585 Pearson, V. and Adrian, M. (2017) Biocontrol of grapevine aerial and root pathogens by *Paenibacillus* sp.
586 strain B2 and paenimyxin in vitro and in planta. Biol. Control 109, 42-50.

587 Ho, S.H., Chen, Y.D., Yang, Z.K., Nagarajan, D., Chang, J.S. and Ren, N.Q. (2017) High-efficiency removal
588 of lead from wastewater by biochar derived from anaerobic digestion sludge. Bioresour. Technol. 246,
589 142-149.

590 Ho, Y.S. (2006) Review of second-order models for adsorption systems. J. Hazard. Mater. 136(3), 681-
591 689.

592 Ho, Y.S. and McKay, G. (1999) Pseudo-second order model for sorption processes. Process Biochem 34(5),
593 451-465.

594 Hu, Q. and Zhang, Z. (2019) Application of Dubinin–Radushkevich isotherm model at the solid/solution
595 interface: A theoretical analysis. J. Mol. Liq. 277, 646-648.

596 Huang, D., Xue, W., Zeng, G., Wan, J., Chen, G., Huang, C., Zhang, C., Cheng, M. and Xu, P. (2016)
597 Immobilization of Cd in river sediments by sodium alginate modified nanoscale zero-valent iron: Impact
598 on enzyme activities and microbial community diversity. Water Res. 106, 15-25.

599 Huang, F., Dang, Z., Guo, C.L., Lu, G.N., Gu, R.R., Liu, H.J. and Zhang, H. (2013) Biosorption of Cd(II) by
600 live and dead cells of *Bacillus cereus* RC-1 isolated from cadmium-contaminated soil. Colloids Surf. B 107,
601 11-18.

602 Huang, F., Guo, C.L., Lu, G.N., Yi, X.Y., Zhu, L.D. and Dang, Z. (2014) Bioaccumulation characterization of
603 cadmium by growing *Bacillus cereus* RC-1 and its mechanism. Chemosphere 109, 134-142.

604 Huang, H., Jia, Q., Jing, W., Dahms, H.U. and Wang, L. (2020) Screening strains for microbial biosorption
605 technology of cadmium. Chemosphere 251, 126428.

606 Ishola, M.M., Isroi and Taherzadeh, M.J. (2014) Effect of fungal and phosphoric acid pretreatment on
607 ethanol production from oil palm empty fruit bunches (OPEFB). Bioresour. Technol. 165, 9-12.

608 Jin, Z., Deng, S., Wen, Y., Jin, Y., Pan, L., Zhang, Y., Black, T., Jones, K.C., Zhang, H. and Zhang, D. (2019)
609 Application of *Simplicillium chinense* for Cd and Pb biosorption and enhancing heavy metal
610 phytoremediation of soils. Sci. Total Environ. 697, 134148.

611 Jin, Z., Xie, L., Zhang, T., Liu, L., Black, T., Jones, K.C., Zhang, H., Wang, X., Jin, N. and Zhang, D. (2020)
612 Interrogating cadmium and lead biosorption mechanisms by *Simplicillium chinense* via infrared
613 spectroscopy. Environ. Pollut. 263(Pt A), 114419.

614 Kaur, S., Rani, S., Mahajan, R.K., Asif, M. and Gupta, V.K. (2015) Synthesis and adsorption properties of
615 mesoporous material for the removal of dye safranin: Kinetics, equilibrium, and thermodynamics. J Ind
616 Eng Chem 22, 19-27.

617 Langmuir, I. (1918) The adsorption of gases on plane surfaces of glass, mica and platinum. J. Am. Chem.
618 Soc.40, 1361-1403.

619 Legatzki, A., Grass, G., Anton, A., Rensing, C. and Nies, D.H. (2003) Interplay of the Czc system and two
620 P-type ATPases in conferring metal resistance to *Ralstonia metallidurans*. J. Bacteriol. 185(15), 4354-
621 4361.

622 Li, F., Wang, W., Li, C., Zhu, R., Ge, F., Zheng, Y. and Tang, Y. (2018) Self-mediated pH changes in culture
623 medium affecting biosorption and biomineralization of Cd²⁺ by *Bacillus cereus* Cd01. J. Hazard. Mater.
624 358, 178-186.

625 Li, H., Lin, Y., Guan, W., Chang, J., Xu, L., Guo, J. and Wei, G. (2010) Biosorption of Zn(II) by live and dead
626 cells of *Streptomyces ciscaucasicus* strain CCNWHX 72-14. J. Hazard. Mater. 179(1-3), 151-159.

627 Masoudzadeh, N., Zakeri, F., Lotfabad, T., Sharafi, H., Masoomi, F., Zahiri, H.S., Ahmadian, G. and
628 Noghabi, K.A. (2011) Biosorption of cadmium by *Brevundimonas* sp. ZF12 strain, a novel biosorbent
629 isolated from hot-spring waters in high background radiation areas. J. Hazard. Mater. 197, 190-198.

630 Mohapatra, R.K., Parhi, P.K., Pandey, S., Bindhani, B.K., Thatoi, H. and Panda, C.R. (2019) Active and
631 passive biosorption of Pb(II) using live and dead biomass of marine bacterium *Bacillus xiamenensis*
632 PbRPSD202: Kinetics and isotherm studies. J. Environ. Manage. 247, 121-134.

633 Nies, A., Nies, D.H. and Silver, S. (1990) Nucleotide sequence and expression of a plasmid-encoded
634 chromate resistance determinant from *Alcaligenes eutrophus*. J. Biol. Chem. 265(10), 5648-5653.

635 NIES, D.H., NIES, A., CHU, L. and SILVER, A.S. (1898) Expression and nucleotide sequence of a plasmid-
636 determined divalent cation efflux system from *Alcaligenes eutrophus*. Proc. Natl. Acad. Sci. U.S.A. 86,
637 7351-7355.

638 Olaniran, A.O., Balgobind, A. and Pillay, B. (2013) Bioavailability of heavy metals in soil: impact on
639 microbial biodegradation of organic compounds and possible improvement strategies. Int. J. Mol. Sci.
640 14(5), 10197-10228.

641 Özdemir, S., Kilinc, E., Poli, A., Nicolaus, B. and Güven, K. (2009) Biosorption of Cd, Cu, Ni, Mn and Zn
642 from aqueous solutions by thermophilic bacteria, *Geobacillus toebii* sub.sp. decanicus and *Geobacillus*
643 *thermoleovorans* sub.sp. stromboliensis: Equilibrium, kinetic and thermodynamic studies. Chem. Eng.J.
644 152(1), 195-206.

645 Ozturk, A. (2007) Removal of nickel from aqueous solution by the bacterium *Bacillus thuringiensis*. J.
646 Hazard. Mater. 147(1-2), 518-523.

647 Peng, D., Qiao, S., Luo, Y., Ma, H., Zhang, L., Hou, S., Wu, B. and Xu, H. (2020) Performance of microbial
648 induced carbonate precipitation for immobilizing Cd in water and soil. J. Hazard. Mater. 400, 123116.

649 Ranjan, D., Talat, M. and Hasan, S.H. (2009) Biosorption of arsenic from aqueous solution using
650 agricultural residue 'rice polish'. J. Hazard. Mater. 166(2-3), 1050-1059.

651 Şahin, Y. and Öztürk, A. (2005) Biosorption of chromium(VI) ions from aqueous solution by the
652 bacterium *Bacillus thuringiensis*. Process Biochem 40(5), 1895-1901.

653 Shi, Z., Qi, X., Zeng, X.A., Lu, Y., Zhou, J., Cui, K. and Zhang, L. (2021) A newly isolated bacterium
654 *Comamonas* sp. XL8 alleviates the toxicity of cadmium exposure in rice seedlings by accumulating
655 cadmium. J. Hazard. Mater. 403, 123824.

656 Sun, F., Sun, W.-L., Sun, H.-M. and Ni, J.-R. (2011) Biosorption behavior and mechanism of beryllium from
657 aqueous solution by aerobic granule. Chem. Eng.J. 172, 783-791.

658 Sun, R., Wang, L., Huang, R., Huang, F., Gan, D., Wang, J., Guan, R., Han, W., Qu, J., Yan, L. and Zhang, Y.
659 (2020) Cadmium resistance mechanisms of a functional strain *Enterobacter* sp. DNB-S2, isolated from
660 black soil in Northeast China. *Environ. Pollut.* 263.

661 Tan, H., Wang, C., Zeng, G., Luo, Y., Li, H. and Xu, H. (2020) Bioreduction and biosorption of Cr(VI) by a
662 novel *Bacillus* sp. CRB-B1 strain. *J. Hazard. Mater.* 386, 121628.

663 Tran, H.N., You, S.-J. and Chao, H.-P. (2016) Thermodynamic parameters of cadmium adsorption onto
664 orange peel calculated from various methods: A comparison study. *J. Environ. Chem. Eng.* 4(3), 2671-
665 2682.

666 Tran, H.N., You, S.J., Hosseini-Bandegharaei, A. and Chao, H.P. (2017) Mistakes and inconsistencies
667 regarding adsorption of contaminants from aqueous solutions: A critical review. *Water Res.* 120, 88-116.

668 Wei, G., Fan, L., Zhu, W., Fu, Y., Yu, J. and Tang, M. (2009) Isolation and characterization of the heavy
669 metal resistant bacteria CCNWS33-2 isolated from root nodule of *Lespedeza cuneata* in gold mine
670 tailings in China. *J. Hazard. Mater.* 162(1), 50-56.

671 Xu, S., Xing, Y., Liu, S., Hao, X., Chen, W. and Huang, Q. (2020) Characterization of Cd²⁺ biosorption by
672 *Pseudomonas* sp. strain 375, a novel biosorbent isolated from soil polluted with heavy metals in
673 Southern China. *Chemosphere* 240, 124893.

674 Yu, Q. and Fein, J.B. (2017) Enhanced Removal of Dissolved Hg(II), Cd(II), and Au(III) from Water by
675 *Bacillus subtilis* Bacterial Biomass Containing an Elevated Concentration of Sulfhydryl Sites. *Environ. Sci.*
676 *Technol.* 51(24), 14360-14367.

677 Zeng, G., Qiao, S., Wang, X., Sheng, M., Wei, M., Chen, Q., Xu, H. and Xu, F. (2021) Immobilization of
678 cadmium by *Burkholderia* sp. QY14 through modified microbially induced phosphate precipitation. *J.*
679 *Hazard. Mater.* 412, 125156.

680 Zhou, W., Liu, D., Zhang, H.o., Kong, W. and Zhang, Y. (2014) Bioremoval and recovery of Cd(II) by
681 *Pseudoalteromonas* sp. SCSE709-6: Comparative study on growing and grown cells. *Bioresour. Technol.*
682 165, 145-151.

683 Zhou, X., Li, H., Liu, D., Hao, J., Liu, H. and Lu, X. (2018) Effects of toxin from *Bacillus thuringiensis* (Bt)
684 on sorption of Pb (II) in red and black soils: equilibrium and kinetics aspects. *J. Hazard. Mater.* 360, 172-
685 181.

686 Zhu, W., Xu, X., Xia, L., Huang, Q. and Chen, W. (2016) Comparative Analysis of Mechanisms of Cd²⁺ and
687 Ni²⁺ Biosorption by Living and Nonliving *Mucoromycote* sp. XLC. *Geomicrobiol. J.* 33(3-4), 274-282.

Supplementary Files

This is a list of supplementary files associated with this preprint. Click to download.

- [SupplementalMaterial10.2.docx](#)